Applied Engineering Letters Vol.7, No.1, 25-31 (2022) e-ISSN: 2466-4847

# THE STUDY OF CHARACTERISTICS OF ELASTICITY AND RESIDUAL STRESSES IN COATINGS APPLIED BY PLASMA METHODS

UDC: 620.198
Original scientific paper https://doi.org/10.18485/aeletters.2022.7.1.4

**Igor Kravchenko[1,2], Ivan Kartsev[1], Sergey Kartsev[1], Sergey Velichko[3], Yury Kuznetsov[4*], Denis Prokhorov[4], Aleksandar Ašonja[5], Larisa Kalashnikova[6]**

[1] Institute of Mechanical Engineering of the Russian Academy of Sciences named after A.A. Blagonravov (IMASH RAS), Moscow, Russia
[2] Russian State Agrarian University – MTAA named after K.A. Timiryazev, Moscow, Russia
[3] National Research Mordovia State University named after N.P. Ogarev, Saransk, Russia
[4] Orel State Agrarian University named after N.V. Parakhin, Orel, Russia
[5] Faculty of Economics and Engineering Management in Novi Sad, University Business Academy in Novi Sad, Serbia
[6] Orel State University named after I.S. Turgenev, Orel, Russia

**Abstract:**
At present, a strategically important task of technological independence of Russian industries is restoration of worn-out parts of machines and equipment by plasma methods based on the use of coatings of different functional purpose. The purpose of this study is to solve the actual problem of choosing the rational modes of plasma coating in the process of restoration of worn parts, subjected to intensive wear in the operation process. To solve this problem, the experimental studies of the elasticity characteristics in the plasma-deposited coatings were carried out. The study results allowed determining the most optimal range of rational modes of plasma coating deposition in terms of obtaining high elastic properties of plasma coatings as the key stage of resource-saving technology for restoration of worn parts of machinery and equipment.

**ARTICLE HISTORY**
Received: 24.01.2022.
Accepted: 10.03.2022.
Available: 31.03.2022.

**KEYWORDS**
Plasma surfacing, Plasmatron, Fatigue resistance, Deformation curve, Fusion zone

## 1. INTRODUCTION

One of the main tasks in the design of technological processes for the restoration of worn items is to determine the rational parameters at which the output parameter would have an optimal value. In practice it is most often required to estimate the parameters, i.e. to build its mathematical model and determine the numerical values of the parameters of this model. In our case it is a technological process of plasma surfacing of wear-resistant coatings. It is known that the bulk of failed parts has wear not exceeding 0.2-0.3 mm. An effective way to restore such items is the plasma surfacing of thin coatings with powder carbide alloys of increased wear resistance [1-7]. At the same time, it is important to select a plasma surfacing mode that would allow applying wear-resistant coatings with minimal resistance to metal fatigue. In this case, the coating retains its original physical and mechanical properties. In order to determine the effect of plasma surfacing modes and surfacing materials on the fatigue resistance of restored parts, it is necessary to establish the elasticity characteristics arising in the coatings applied by plasma methods, as well as the residual stresses in the fusion zone [8-15].

## 2. MATERIALS AND METHODS

To conduct experimental studies, samples were made, which were the rings of steel grade 40G with

*CONTACT: Y. Kuznetsov, e-mail: kentury@yandex.ru 

an outer diameter of 55 mm, inner - 35 mm and a width of 10 mm. Plasma surfacing was performed along the outer diameter of the sample with the powdered material composition [16]. In this case, the constant parameters during plasma surfacing were:

- plasmatron vibration amplitude - $A$ = 18 mm;
- plasmatron oscillation frequency - $v$ = 80 min$^{-1}$;
- plasma gas flow rate - $g_1$ = 1.5-1.8 l/min;
- conveying gas flow rate - $g_2$ = 10-12 l/min.

The hardness of coated samples was determined by non-destructive expressive measurement using a universal programmable electronic portable hardness tester TEMP-4 (ТЭМП-4). The hardness tester allows to work in any standardized scale: Brinell (*HB*), Rockwell (*HRC$_e$*), Shore (*NSD*), Vickers (*HV*), since the values obtained by the different methods are connected with certain dependencies. Before measurements, the hardness tester was calibrated using standard hardness measures tested on state hardness standards according to Brinell, Vickers, Rockwell and Shore scales, which ensured high accuracy of measurements [17, 18]. The ranges of hardness measurements on the scales are given in Table 1.

The compact portable hardness tester TEMP-4 (ТЭМП-4) provides rapid hardness testing of almost any surface and in any direction. The procedure for hardness testing with the TEMP-4 portable hardness tester is shown in Fig.1.

**Table 1.** Hardness measurement ranges according to scales

| Scale | Indicator | Designation |
|---|---|---|
| Rockwell | 22-68 | HRCe |
| Brinell | 100-450 | HB |
| Shore | 22-99 | HSD |
| Vickers | 100-950 | HV |

**Fig. 1.** Portable hardness tester TEMP-4 (ТЭМП-4)

The hardness was measured on the Vickers scale at four opposite sample points and the average value was taken. The ring inner diameter was measured before and after the plasma surfacing in perpendicular planes with three measurements in each plane and the average value was taken. The difference between the measurements before and after plasma surfacing was used to determine the shrinkage. In this case, the modes of plasma surfacing rings and the results of measurements are presented in Table 2.

**Table 2.** Modes of plasma surfacing of samples

| Samples | Plasmatron arc current *I*, A | Plasmatron arc voltage *U*, B | Plasmatron travel speed *V*, m/min | *Al*, % | Hardness, *HV* | Coating thickness *h*, mm | Shrinkage, mm |
|---|---|---|---|---|---|---|---|
| 1 | 200 | 53 | 0.34 | 8 | 583 | 1.10-1.20 | 0.15 |
| 2 | 200 | 53 | 0.14 | 8 | 580 | 1.20-1.40 | 0.36 |
| 3 | 140 | 48 | 0.34 | 8 | 565 | 1.10-1.15 | 0.13 |
| 4 | 140 | 48 | 0.14 | 8 | 572 | 1.10-1.30 | 0.28 |
| 5 | 200 | 53 | 0.24 | 14 | 566 | 1.20-1.30 | 0.27 |
| 6 | 200 | 53 | 0.24 | 2 | 570 | 1.30-1.40 | 0.31 |
| 7 | 140 | 48 | 0.24 | 14 | 517 | 1.30-1.40 | 0.17 |
| 8 | 140 | 48 | 0.24 | 2 | 570 | 1.80-2.00 | 0.22 |

To optimize the plasma deposition parameters, the method of complete factor experiment was applied [19-21]. The Young's modulus was adopted as the optimization criterion [22-24]. Taking into account the information about the influence of individual factors in plasma surfacing on the optimization criterion, the levels and intervals of variation of the main factors that have the most significant influence on the physical and mechanical properties of the applied coatings were selected. The matrix of variation of plasma surfacing modes is presented in Table 3.

**Table 3.** Matrix of variation of plasma surfacing modes

| Name | *I*, A (*X₁*) | *V*, m/min (*X₂*) | *Al*, % (*X₃*) |
|---|---|---|---|
| Basic level | 170 | 0.24 | 8 |
| Variation interval | 30 | 0.10 | 2 |
| Upper level | 200 | 0.34 | 10 |
| Lower level | 140 | 0.14 | 6 |

The elasticity characteristics were investigated in the following sequence. Six consecutive ring diameters (56.5; 55.5; 54.5; 53.5; 52.5 and 51.5 mm) with plasma surfacing coatings were performed on a turning lathe. After each turning, the weight of the remaining sample was measured on a laboratory scale VLA-200 with an accuracy of 0.01 g; the outer diameter of the rings was measured with a micrometer with an accuracy of 0.01 mm, the resonance frequency of oscillations and the cross-section stiffness of the studied sample was calculated according to the obtained data. As a result of the experiment, the dependence of the ring stiffness $B$ on its axial moment of inertia $J_x$ was established, and this can be represented by the expression:

$$\boldsymbol{E} = \frac{\boldsymbol{dB}}{\boldsymbol{dJ_x}} \tag{1}$$

The obtained dependence can be approximated, and then the derivative of this function will give us the value of the Young's modulus $E$ in any coating applied by plasma surfacing and in the base metal. To determine the resonant frequency of the bending vibrations, a circular sample was placed between two piezoelectric elements, one of which is designed to emit sound frequency vibration, and the other serves as a receiver. The transmitter was connected to an oscillator designed to change its frequency. By changing the frequency of the ring forced oscillation, its value is brought to coincidence with the ring natural frequency. By a sharp increase in the oscillations amplitude of the sample, the resulting resonance was recorded on the oscilloscope screen. The exact value of the oscillations resonance frequency was measured with a frequency meter. The bending stiffness function of the ring is a curve, which indicates that the elastic modulus change in thickness [25]. In the surface layers of coatings applied by plasma surfacing, the elastic moduli have a reduced value. As they move deeper into the surfaced coating, they increase, and in the fusion zone with the base metal, they decrease again. In the base metal, the modulus of elasticity remain constant. The values of elastic modulus in the coatings applied by plasma surfacing and in the fusion zone for all the tested samples are shown in Table 4. The Young's modulus $E$ of the base material for all the examined samples was 1.92×10$^4$ MPa.

**Table 4.** Elastic moduli of the coatings applied by plasma surfacing and the fusion zone with the base metal

| Samp-les | Young's modulus *E* 10$^4$ , MPa of coating at sample thickness, mm | | | | | | | |
|---|---|---|---|---|---|---|---|---|
| 1 | 11.25 | 10.95 | 10.65 | 10.35 | 9.95 | 9.55 | 9.15 | 8.65 |
| 2 | 1.36 | 1.46 | 1.52 | 1.53 | 1.61 | 1.85 | 1.40 | 1.33 |
| 3 | 1.86 | 1.34 | 1.92 | 2.14 | 2.00 | 1.91 | 1.40 | 1.37 |
| 4 | 1.56 | 1.53 | 1.43 | 1.66 | 1.66 | 1.55 | 1.91 | 1.36 |
| 5 | 1.42 | 1.52 | 1.51 | 1.61 | 1.78 | 1.57 | 1.43 | 1.38 |
| 6 | 1.46 | 1.59 | 1.33 | 1.48 | 1.63 | 1.56 | 1.41 | 1.40 |
| 7 | 1.86 | 1.41 | 1.49 | 1.68 | 1.58 | 1.40 | 1.41 | 1.35 |
| 8 | 1.93 | 1.07 | 1.14 | 1.28 | 1.38 | 1.32 | 1.48 | 1.38 |

## 3. RESULTS AND DISCUSSION

The analysis of the obtained study results demonstrated that the change in the elasticity characteristics is significantly influenced by the plasma surfacing modes. As a result of mathematical processing of the results of the experiments performed in the sequence specific for the method of planning a complete factor experiment [26-27], a mathematical model in the form of a regression equation was obtained:

$$\hat{Y} = \mathbf{1.48} + \mathbf{0.10}\boldsymbol{X_1} - \mathbf{0.115}\boldsymbol{X_2} - \mathbf{0.15}\boldsymbol{X_3} + \mathbf{0.22}\boldsymbol{X_1^2} + \mathbf{0.17}\boldsymbol{X_2^2} - \mathbf{0.10}\boldsymbol{X_3^2} \tag{2}$$

and adequately describes the field of experimentation (variance of adequacy $S_{ad^2} = 0.0093$, dispersion of experience $S_{y^2} = 0.0052$, the calculated Fisher criterion is $F_p = 1.79$, tabular – $F_T = 19.3$) and allows the estimation of the cumulative effect of plasma surfacing modes on the maximum values of their elastic moduli.

For practical calculations, the resulting regression equation is more convenient in the transformed form. After appropriate transformations in the natural scale it will take the final form:

$$\boldsymbol{E} = (\mathbf{9.484} - \mathbf{0.080}\boldsymbol{I} - \mathbf{9.31}\boldsymbol{V} + \mathbf{0.175}\boldsymbol{Al} + \mathbf{2.44} \cdot \mathbf{10^{-4}}\boldsymbol{I^2} + \mathbf{17}\boldsymbol{V^2} - \mathbf{0.025}\boldsymbol{Al^2}) \cdot \mathbf{10^4}\ \text{, MPa} \quad (3)$$

Graphical interpretation of the dependence of the optimization criterion E on the varying factors that have a significant effect on the physical and mechanical properties of the applied coatings is shown in Fig.2.

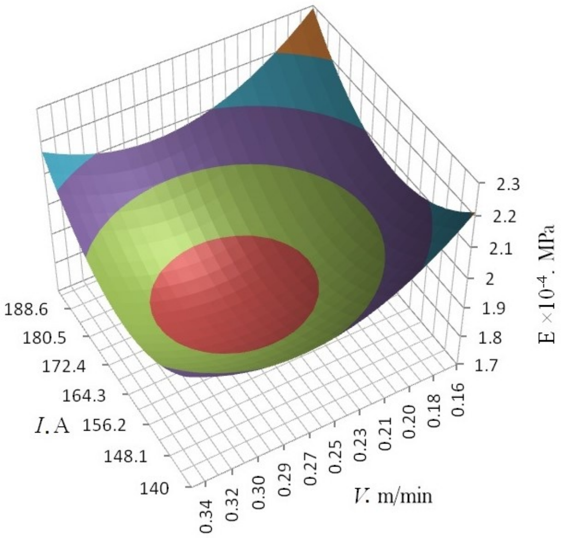


**Fig. 2.** Dependence of Young's modulus $\boldsymbol{E}$ on arc current of plasmatron I, its travel speed $\boldsymbol{V}$ at constant values of voltage $\boldsymbol{U}$ = 48 V and aluminum $\boldsymbol{Al}$ content in composite powder material 8%

The most optimal in terms of obtaining high elastic properties is the plasma surfacing mode, at which $I = 170$ A, $U = 48$ V, $V = 0.14$ m/min. At the same time, the powdered aluminum content in the composite powder material was 8% [28]. It should be noted that the highest hardness of the surfaced coating, which was $HV = 580$ was obtained in this plasma surfacing mode.

The samples for determining the elasticity characteristics were used as samples for determining residual stresses [29].

Residual stresses were calculated using the following methodology:

1. The coated samples were consistently turned on the lathe in a special fixture and after each turning the circumferential stains were recorded. Strain measurements were carried out using strain gauges at two points on the circumference. Strain gauges on the samples were fixed with glue. To measure the rings strains, an electrical circuit was assembled, which included the working and compensation rings under study with glued electronic sensors measuring statistical strains. Measurements were taken after each turning and coating layers removal.

2. Based on the obtained and processed experimental data using statistical methods, the strain curve $\varepsilon_b(r)$ was plotted. When developing a method for plotting the calculated conditional strain curve in the presence of characteristic values, one of the requirements for its schematization is that the schematization parameters can be selected by comparing them with experimental strain curves (Fig.3).

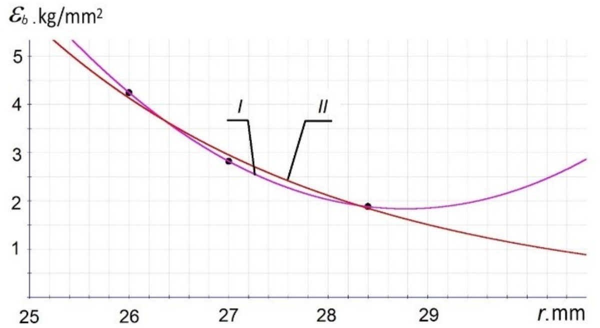


**Fig. 3.** Strain curves: *I* – experimental, *II* -conventional

The accuracy of the resulting curve directly depends on the number and quality of the primary experimental strain curves [30].

According to the results of this research, an approach to the construction of calculated conditional strain curves consisting of four sections has been developed:

- the first section is linear by points;
- the second section is the spline between the points;
- the third section is the section of a sharp rise in the curve between points, which is described by the logarithmic function;
- the fourth section is the hardening section described by a fourth-order polynomial.

It should be noted that in the case of a large number of experimental strain curves, it is advisable to follow the MMPDS requirements for the design curves plotting [30].

3. The residual circumferential stresses were determined from the following expression:

$$\sigma_{\text{в}} = -\frac{AK(r)+B(r)D}{4R_2^2 r}\frac{d\varepsilon_b}{dr} - \frac{E_1 A91+\mu_2}{2R_2^2}\varepsilon_b(r) + \frac{AK(r)+B(r)d}{4R_2^2 r}\varepsilon_b(r) \quad (4)$$

$$A = (1-\mu_1)R_2^2 + (1+\mu_2)R_1^2 \quad (5)$$

$$K(r) = E_2(r^2 - R_2^2) \quad (6)$$

$$B(r) = (1-\mu_2)R_2^2 + (1+\mu_2)r^2 \quad (7)$$

$$D = E_1(R_2^2 - R_1^2) \quad (8)$$

Where:

$R_1$, $R_2$, $r$ – respectively the radius of the ring inner surface, the ring-coating interface and the current radius ($R_2 \leq r \leq R_1$);

$E_1$, $E_2$ – elastic moduli of the inner and outer parts of the ring;

$\mu_1$, $\mu_2$ – respectively Poisson's coefficients for these parts.

The values of residual stresses $\sigma_b$ in the coatings applied by plasma surfacing to the samples, depending on the value of the variable radius $r$, are presented in Table 5. Note that the radial residual stresses are quite insignificant and can be neglected.

**Table 5.** Residual stresses in the coating layers applied by plasma surfacing depending on the value of the variable radius *r*

| Sample number | Ring radius *r*, mm | *σ<sub>в</sub>*, kg/mm² | Sample number | Ring radius *r*, mm | *σ<sub>в</sub>*, kg/mm² | Sample number | Ring radius *r*, mm | *σ<sub>в</sub>*, kg/mm² |
|---|---|---|---|---|---|---|---|---|
| 1 | 28.40 | 4.24 | 3 | 28.35 | 19.37 | 5 | 28.00 | 10.50 |
| | 27.00 | 2.82 | | 27.00 | 13.52 | | 27.00 | 3.80 |
| | 26.00 | 1.88 | | 26.00 | 10.26 | | 26.00 | 1.79 |
| 2 | 28.00 | 3.05 | 4 | 27.50 | 4.59 | 6 | 28.35 | -6.84 |
| | 27.00 | 7.54 | | 26.00 | 5.44 | | 27.00 | 2.73 |
| | 26.00 | 8.20 | | 25.00 | 5.84 | | 26.00 | 3.11 |

The results of the analysis of the obtained data show that in almost all cases (except for sample No. 6) there are circumferential tensile stresses on the surface. The main reasons for their occurrence are the uneven cooling in the process of plasma surfacing and the nature of the structures of the surfaced coatings.

## 4. CONCLUSION

The key research results in this paper are as follows:

1. Tensile stresses that reduce fatigue resistance are formed in the surfaced coating during plasma surfacing with powder composite alloys. Fatigue resistance of the parts restored by plasma surfacing with the given alloys decreased by 20-25% from the maximum worn parts level.

2. The carried-out researches on optimization of plasma surfacing by the method of full multifactorial experiment allowed establishing the optimization criteria which is most influenced by the plasma surfacing speed and oscillation amplitude. Relative wear resistance of coatings surfaced with powder hard alloys is 3-5 times higher in comparison with hardened steel 45. At the same time the addition of 8% aluminum powder to the initial powder hard alloys provides the increase in their wear resistance

3. The results of the study to determine the elasticity characteristics and residual stresses in the coating demonstrated that in the surface layers of the surfaced coatings, the elastic moduli have reduced values and tensile residual stresses arise.

## REFERENCES

[1] S.A. Sidorov, D.A. Mironov, V.K. Khoroshenkov, E.I. Khlusova, Surfacing methods for increasing the service life of rapidly wearing working tools of agricultural machines. *Welding International*, 30(10), 2016: 808-812. https://doi.org/10.1080/09507116.2016.1148408

[2] B. Huang, Ch. Zhang, G. Zhang, H. Liao, Wear and corrosion resistant performance of thermal-sprayed Fe-based amorphous coatings: A review. *Surface and Coatings Technology*, 377, 2019: 124896. https://doi.org/10.1016/j.surfcoat.2019.124896

[3] M. AE. Hafez, S.A. Akila, M.A. Khedr, A.S. Khalil, Improving wear resistance of plasma-sprayed calcia and magnesia-stabilized zirconia mixed coating: roles of phase stability and microstructure. *Scientific Reports*, 10, 2020: 21830. https://doi.org/10.1038/s41598-020-78088-6

[4] G. Mauer, M.O. Jarligo, D.E. Mack, R. Vaßen, Plasma-sprayed thermal barrier coatings: new materials, processing issues, and solutions, *Journal of Thermal Spray Technology*, 22(5), 2013: 646-658. https://doi.org/10.1007/s11666-013-9889-8

[5] V. Alisin, R.N. Roshchin, Thermal plasma spray to protect large-size parts of friction joints against wear. *Solid State Phenomena*, 316, 2021: 770-776. https://doi.org/10.4028/www.scientific.net/SSP.316.770

[6] P.V. Gladkii, E.F. Perepletchikov, I.A. Ryabtsev, Plasma surfacing. *Welding International*, 21(9), 2007: 685-693. https://doi.org/10.1080/09507110701631141

[7] O. N. Çelik, Microstructure and wear properties of WC particle reinforced composite coating on Ti6Al4V alloy produced by the plasma transferred arc method. *Applied Surface Science*, 274(6), 2013: 334-340. https://doi.org/10.1016/j.apsusc.2013.03.057

[8] Yi. Wei, Xian-sh. Wei, B. Chen, Ji.-yo. Zuo, Tian cai. Ma, Jun Shen, Parameter optimization for tungsten carbide/Ni-based composite coating deposited by plasma transferred arc hardfacing. *Transactions of Nonferrous Metals Society of China*, 28(12), 2018: 2511-2519. https://doi.org/10.1016/S1003-6326(18)64897-6

[9] L.-M. Berger, Application of hardmetals as thermal spray coatings. *International Journal of Refractory Metals and Hard Materials*, 49(3), 2015: 350-364. https://doi.org/10.1016/j.ijrmhm.2014.09.029

[10] P. Fauchais, G. Montavon, G. Bertrand, From powders to thermally sprayed coatings. *Journal of Thermal Spray Technology*, 19, 2010: 56-80. https://doi.org/10.1007/s11666-009-9435-x

[11] S.M. Muneer, M. Nadeera, Wear characterization and microstructure evaluation of silicon carbide based nano composite coating using plasma spraying. *Materials Today: Proceedings*, 5(11), part 3, 2018: 23834-23843. https://doi.org/10.1016/j.matpr.2018.10.175

[12] Zh. Gan, Heong W. Ng, Ap. Devasenapathi, Deposition-induced residual stresses in plasma-sprayed coatings. *Surface and Coatings Technology*, 187(2-3), 2004: 307-319. https://doi.org/10.1016/j.surfcoat.2004.02.010

[13] W. Tillmann, L. Hagen, W. Luo, Process parameter settings and their effect on residual stresses in WC/$W_2C$ reinforced iron-based arc sprayed coatings. *Coatings*, 7(8), 2017: 125. https://doi.org/10.3390/coatings7080125

[14] S.-W. Yao, J.-J. Tian, C.-J. Li, G.-J. Yang, C.-X. Li, Understanding the formation of limited interlamellar bonding in plasma sprayed ceramic coatings cased on the concept of intrinsic bonding temperature. *Journal of Thermal Spray Technology*, 25(8), 2016: 1617-1630. https://doi.org/10.1007/s11666-016-0464-y

[15] I.N. Kravchenko, S.V. Kartsev, Yu.A. Kuznetsov, S. A. Velichko, Optimization of plasma deposition and coating plasma fusion parameters and regimes. *Refractories and Industrial Ceramics*, 62(1), 2021: 51-56. https://doi.org/10.1007/s11148-021-00557-w

[16] I.N. Kravchenko, S.V. Kartsev, Yu.A. Kuznetsov, Use of hot hydrocarbons in a plasma installation for application of wear-resistant coating. *Refractories and Industrial Ceramics*, 61(4), 2020: 399-403. https://doi.org/10.1007/s11148-020-00492-2

[17] G. Dwivedi, T. Wentz, S. Sampath, T. Nakamura, Assessing process and coating reliability through monitoring of process and design relevant coating properties. *Journal of Thermal Spray Technology*, 19(6), 2010: 695-712. https://doi.org/10.1007/s11666-009-9467-2

[18] D. Chicot, H. Ageorges, M. Voda, G. Louis, M.A. Ben Dhia, C.C. Palacio, S.Kossman, Hardness of thermal sprayed coatings: Relevance of the scale of measurement. *Surface and Coatings Technology*, 268(4), 2015: 173-179. https://doi.org/10.1016/j.surfcoat.2014.04.043

[19] O.P. Solonenko, V.I. Jordan, V.A. Blednov, Stochastic computer simulation of cermet coatings formation. *Advances in Materials Science and Engineering*, 2015: 396427. https://doi.org/10.1155/2015/396427

[20] B.A. Okovitiy, F.I. Panteleenko, V.V. Okovitiy, V.M. Astashinsky, Optimization of the process of coating deposition of metal-ceramic powders by plasma spraying in air. *Science and Technology,* 20(5), 2021: 369-374. https://doi.org/10.21122/2227-1031-2021-20-5-369-374

[21] I. Ahmed, T.L. Bergman, Optimization of plasma spray processing parameters for deposition of nanostructured powders for coating formation. *Journal of Fluids Engineering*, 128(2), 2006: 394-401. https://doi.org/10.1115/1.2170131

[22] D. Thirumalaikumarasamy, V. Dalasubramanian, S. Sree Sabari, Prediction and optimization of process variables to maximize the Young's modulus of plasma sprayed alumina coatings on AZ31B magnesium alloy. *Journal of Magnesium and Alloys*, 5(1), 2017: 133-145. https://doi.org/10.1016/j.jma.2017.02.002

[23] J. H. You, T. Höschen, S. Lindig, Determination of elastic modulus and residual stress of plasma-sprayed tungsten coating on steel substrate. *Journal of Nuclear Materials*, 348(1-2), 2006: 94-101. https://doi.org/10.1016/j.jnucmat.2005.09.015

[24] W.C. Oliver, G.M. Pharr, Measurement of hardness and elastic modulus by instrumented indentation: Advances in understanding and refinements to methodology. *Journal of Materials Research*, 19(1), 2004: 3-20. https://doi.org/10.1557/jmr.2004.19.1.3

[25] A.B. Vakhrushev, A.A. Pushkov, S.N. Zykov, and V.S. Klekovkin, Determination of the Young modulus of nanoparticles based on numerical simulation and experimental studies. P.1. Methodological foundations of numerical simulations. *Chemical Physics and Mesoscopy*, 16(3), 2014: 381-387.

[26] R.C. Batra, U. Taetragool, Numerical techniques to find optimal input parameters for achieving mean particles' temperature and axial velocity in atmospheric plasma spray process. *Scientific Reports*, 10, 2020: 21483. https://doi.org/10.1038/s41598-020-78424-w

[27] M. A. Ageev, T.V. Vigerina, K.A. Danko, S.A. Dovzhuk, S.L. Chigray, A.V. Lopata, Assessment of influence of parameters of gas-thermal spraying of coatings on their properties by using mathematical planning methods. *Bulletin of Polotsk State University. Series V. Industry. Applied Sciences*, 3, 2017: 35-40.

[28] I.N. Kravchenko, S.V. Kartsev, A.V. Kolomeichenko, Yu.A. Kuznetsov, S.N. Perevislov, M.A. Markov, Metallurgical features of plasma surfacing with powder hard alloy with addition of aluminum powder. *Metallurgist*, 64(9-10), 2021: 1077-1085. https://doi.org/10.1007/s11015-021-01089-x

[29] C.V. Kartsev, Mathematical model of optimization of controllable parameters of the technological process of plasma surfacing of wear-resistant coatings. *Problems of Mechanical Engineering and Automation*, 2, 2020: 50-55.

[30] B.E. Vasilyev, M.E. Volkov, E.N. Bredihina, I.I. Pleshcheev, Plotting of calculated deformation curves to provide a data bank on the structural strength of aircraft engine materials. *Materials Physics and Mechanics*, 42(5), 2019: 656-670.

[31] MMPDS-11: Metallic materials properties development and standardization (MMPDS). Battelle Memorial Institute, 2016.